Research Square

Preprints are preliminary reports that have not undergone peer review.
They should not be considered conclusive, used to inform clinical practice,
or referenced by the media as validated information.

The Mesh-Insensitive Structural Stress Method: Current State and Prospects for Additively Manufactured Components

Pingsha DONG

dongp@umich.edu

University of Michigan https://orcid.org/0000-0003-3265-858X

Research Article

Keywords: Welded structures, mesh-insensitive structural stress, master S–N curve, finite element, ASME code, fatigue, low-cycle fatigue, metal AM

Posted Date: November 6th, 2026

DOI: https://doi.org/10.21203/rs.3.rs-11334392/v1

License: This work is licensed under a Creative Commons Attribution 4.0 International License.
Read Full License

The Mesh-Insensitive Structural Stress Method: Current State and Prospects for Additively Manufactured Components

Pingsha Dong
Department of Naval Architecture and Marine Engineering
The University of Michigan
Ann Arbon, Michigan, USA
dongp@umich.edu

Abstract

Fatigue failure in welded structures is strongly influenced by stress concentration, which in turn depends on plate thickness, loading mode, weld geometry, among others. Traditional fatigue assessment approaches, such as nominal stress, hot-spot stress, and effective notch stress methods, have been applied in design codes and engineering practice, but they can become difficult to apply consistently to complex welded structures. One major issue is how to suppress mesh-size sensitivity in finite element models. The mesh-insensitive structural stress method has been shown as an effective alternative method since its adoption by the ASME Boiler and Pressure Vessel Code since 2007. The method leads to the master S–N curve approach, which correlates fatigue data from a wide range of welded joint types using a unified fatigue curve and scatter band. This paper reviews the mechanics foundation, finite-element implementation, current engineering applications, advantages, limitations, and on-going development in the area of low cycle fatigue, and applications for fatigue evaluation of additively manufactured metal components.

Keywords: Welded structures; mesh-insensitive structural stress; master S–N curve; finite element; ASME code; fatigue; low-cycle fatigue; metal AM

1. INTRODUCTION

Welded structures are widely used in pressure vessels, ship and offshore structures, bridges, railway vehicles, automobiles, heavy equipment, pipelines, and many other engineering systems. Although welding provides an efficient and economical means of joining structural components, welded joints are often fatigue-critical locations under cyclic loading. Fatigue cracks commonly originate at weld toes, weld roots, or other local discontinuities where stress concentration is severe.

Historically, fatigue assessment of welded structures has relied heavily on nominal stress-based S–N curves [1], [2], [3]. In this approach, a welded detail is classified into a fatigue category, and fatigue life is estimated using the nominal stress range away from the local weld discontinuity. Nominal stress methods remain widely used because of their simplicity and their long history in design codes. However, they can become difficult to apply when welded details are complex, when the load path is three-dimensional, or when the nominal stress is not clearly defined.

To overcome some of these limitations, more local approaches such as the hot-spot stress method [4], [5], [6] and effective notch stress method [7] have been developed. The hot-spot stress method uses extrapolated surface stresses near the weld toe to account for structural stress concentration, while excluding the local weld notch effect. The effective notch stress method explicitly models a reference weld toe or root notch radius and evaluates the local notch stress. These methods are useful, but they introduce their own difficulties. Hot-spot stress results depend on finite element mesh design and stress extrapolation rules, while effective notch stress analysis requires detailed local geometry and very fine finite element (FE) model meshes.

A central problem in finite-element-based fatigue assessment is therefore mesh-size sensitivity. In a finite element model, the local stress near an idealized sharp weld toe or root can increase as the mesh is refined. This occurs because the weld toe or root may behave mathematically as a stress singularity. If fatigue life is calculated directly from such local stresses, the prediction may depend more on mesh size than on the actual structural behavior.

The mesh-insensitive structural stress method, developed primarily through the work of Dong and co-workers [8], [9], [10], was introduced to address this problem. The method defines a weld-line structural stress based on equilibrium-equivalent nodal forces and moments rather than directly using local finite element stresses. The structural stress is decomposed in statically equivalent manner into membrane and bending components across plate thickness section, which are consistent with principles of structural mechanics. As a result, the calculated through-thickness structural stress is much less sensitive to mesh size than conventional local stress quantities.

The method further leads to the master S–N curve approach [11], in which fatigue data from a wide range of welded joint types can be represented using a unified fatigue curve and scatter band. Since its adoption into the ASME Boiler and Pressure Vessel Code, Section VIII, Division 2, in 2007[12], the method has become an important fatigue assessment tool for pressure vessels and other welded structures.

This paper provides an overview of the mesh-insensitive structural stress method for welded structures. The discussion is organized into the following sections: introduction, mechanics basis of the mesh-insensitive method, master S–N curve definition and usage, applications, on-going and future development, and conclusions.

2. MECHANICS BASIS AND FINITE ELEMENT IMPLEMENTATION

2.1 Stress Decomposition at Welded Joints

The basic idea is that the fatigue-relevant stress at a weld location, e.g., at weld toe (or weld root), can be represented by a statically equivalent membrane and bending stress components across hypothetical crack path in fracture mechanics context, as illustrated in Figure 1[9]. Here f and m represents internal force and moments (per unit length into the paper) along the hypothetical free body cut on which transverse for V is assumed negligible for simplicity. In terms of its membrane and bending parts also referred to as the linear traction stress, the structural stress σ_s can be expressed as:

$$\sigma_s = \frac{f}{t} + \frac{6m}{t^2} = \sigma_m + \sigma_b \tag{1}$$

where σ_m is the membrane stress component and $\sigma_b$is the bending stress component. In fatigue evaluation of welded components, the stress range is typically used, i.e., $\Delta\sigma_s = \Delta\sigma_m + \Delta\sigma_b$

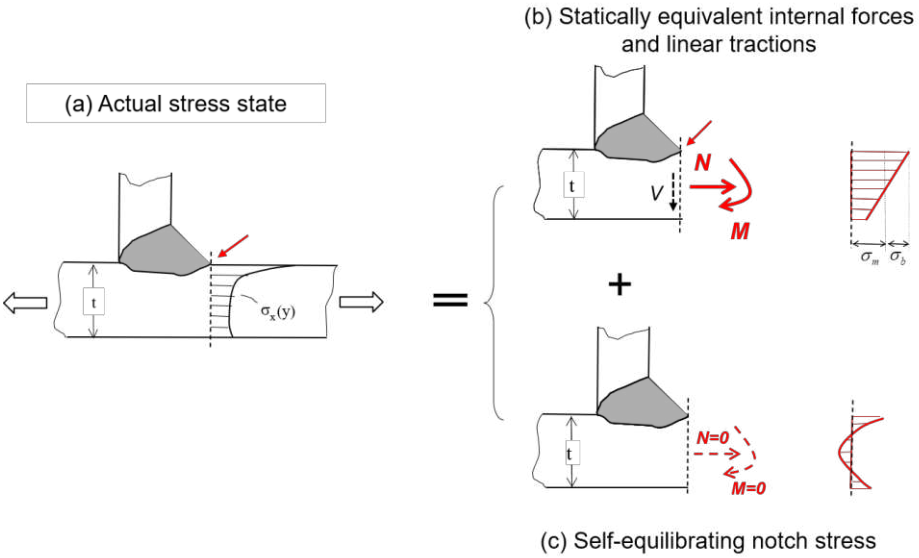


Figure 1: Traction-based structural stress definiton

2.2 Two-Dimensional Calculation Procedure

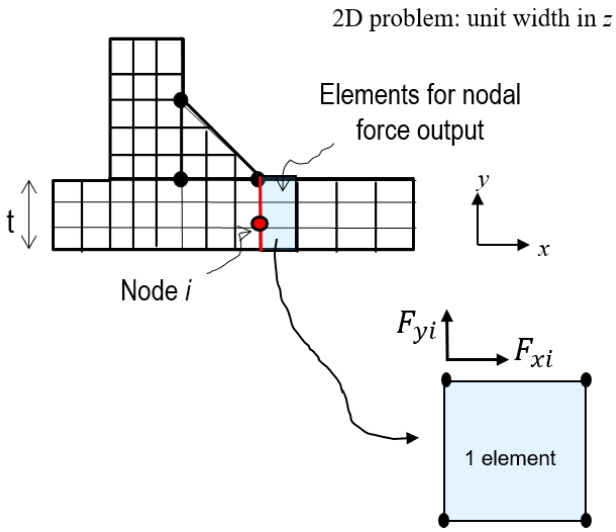


Figure 2: 2D structural stress calculation procedure

For two-dimensional (2D) stress concentration problems associated with welded joints, e.g., a T fillet weld as shown in Figure 2. The structural stress can be simply calculated by considering a

free-body cut along the red line by collecting nodal forces with respect to the three elements on the right (i.e., shaded elements). Then, the statically equivalent membrane and bending stress components can be calculated by:

$$\sigma_m = \frac{1}{t}\sum_{i=1}^{n} F_{xi}$$
$$\sigma_b = \frac{6}{t^2}\sum_{i=1}^{n} F_{xi} \times (y_i - t/2) \qquad (2)$$

A cover-plate fillet weld specimen is considered in Figure 3a. Two representative FE model with different element sizes are illustrated in Figure 3b. It is evident that the structural stress concentration factor (defined as the calculated structural stress divided by remote nominal stress (F/A)) is essentially constant, as shown in Figure 3c.

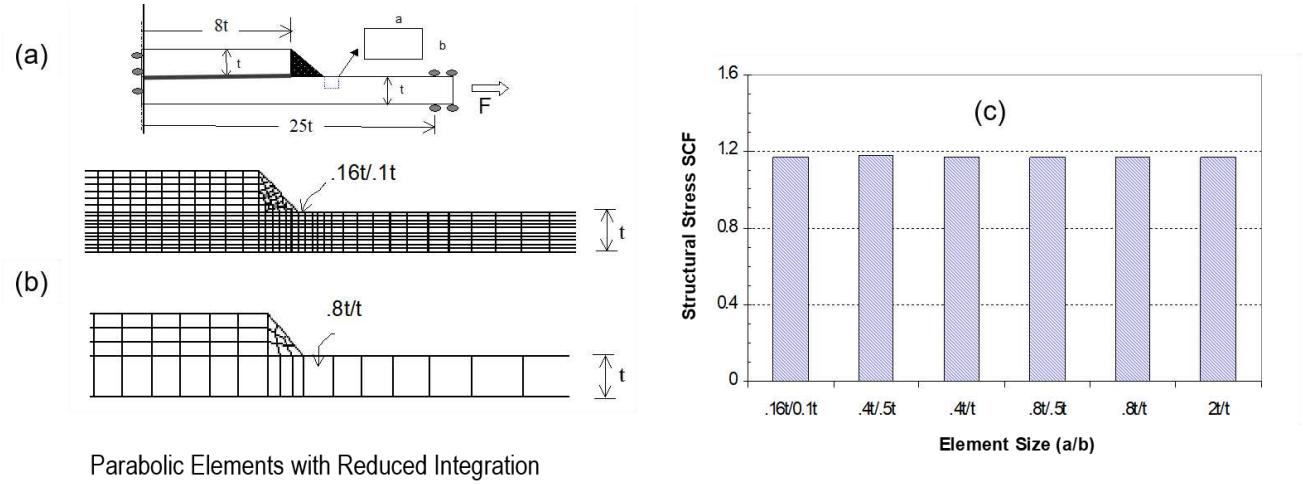


Figure 3: Validation of mesh-size sensitivity of Eq. (2) – single cover-plate fillet weld under tension

2.3 3D calculation procedure

Consider an arbitrarily curved weld in space with weld toe position defined by nodal numbering N_1 through N_i in Figure 4 in which shell or plate element model is assumed without losing generality. With respect to the local ordinate system (x', y', z'), the rotated nodal force and moment vectors versus nodal line force and moment vectors can be related in matrix equation form as:

$$\{F\}_{y'} = [A]\{f\}_{y'}$$
$$\{M\}_{x'} = [A]\{m\}_{x'} \qquad (3)$$

in which, [*A*] matrix is given as [9] for closed weld line:

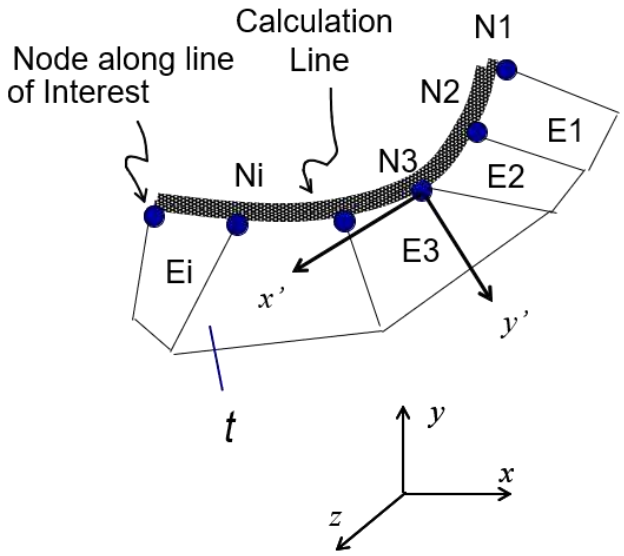


Figure 4: 3D Structural Stress Calcualtion Procedure

$$[A]=\begin{bmatrix} \frac{(l_1+l_{n-1})}{3} & \frac{l_1}{6} & 0 & 0 & \cdots & \frac{l_{n-1}}{6} \\ \frac{l_1}{6} & \frac{(l_1+l_2)}{3} & \frac{l_2}{6} & 0 & \cdots & 0 \\ 0 & \frac{l_2}{6} & \frac{(l_2+l_3)}{3} & \frac{l_3}{6} & 0 & \vdots \\ 0 & 0 & \ddots & \ddots & \ddots & 0 \\ \vdots & \ddots & 0 & \frac{l_{n-3}}{6} & \frac{(l_{n-3}+l_{n-2})}{3} & \frac{l_{n-2}}{6} \\ \frac{l_{n-1}}{6} & \cdots & 0 & 0 & \frac{l_{n-2}}{6} & \frac{(l_{n-2}+l_{n-1})}{3} \end{bmatrix} \quad (4)$$

In Eq. (4), $l_1, \ldots, l_i$ represents element length between $N_1$and N_2, …, N_i and N_{i+1}, respectively. The resulting structural stress at each nodal location can then be calculated from:

$$\sigma_s = \sigma_m + \sigma_b = \frac{\mathrm{f}_{y'}}{\mathrm{t}} - \frac{6m_{x'}}{\mathrm{t}^2} \quad (5)$$

Note that the minus operator in Eq. (5) is due to the fact that a positive moment $m_{x'}$ produces negative (i.e., compressive) bending stress with respect to the local coordinate system, as shown in Figure 4.

With the above structural stress calculation procedure, the mesh-insensitivity can be clearly seen when used for a complex welded connection [13] between two hollow connection shown in Figure 5, a blind Weld Challenge fatigue problem organized by SAE Fatigue Design & Evaluation Committee in 2004. The predicted failure location in Figure 5c is consistent with the experimental observations over about 10 tests on the same specimen. Further details can be found in Kyuba and Dong [13].

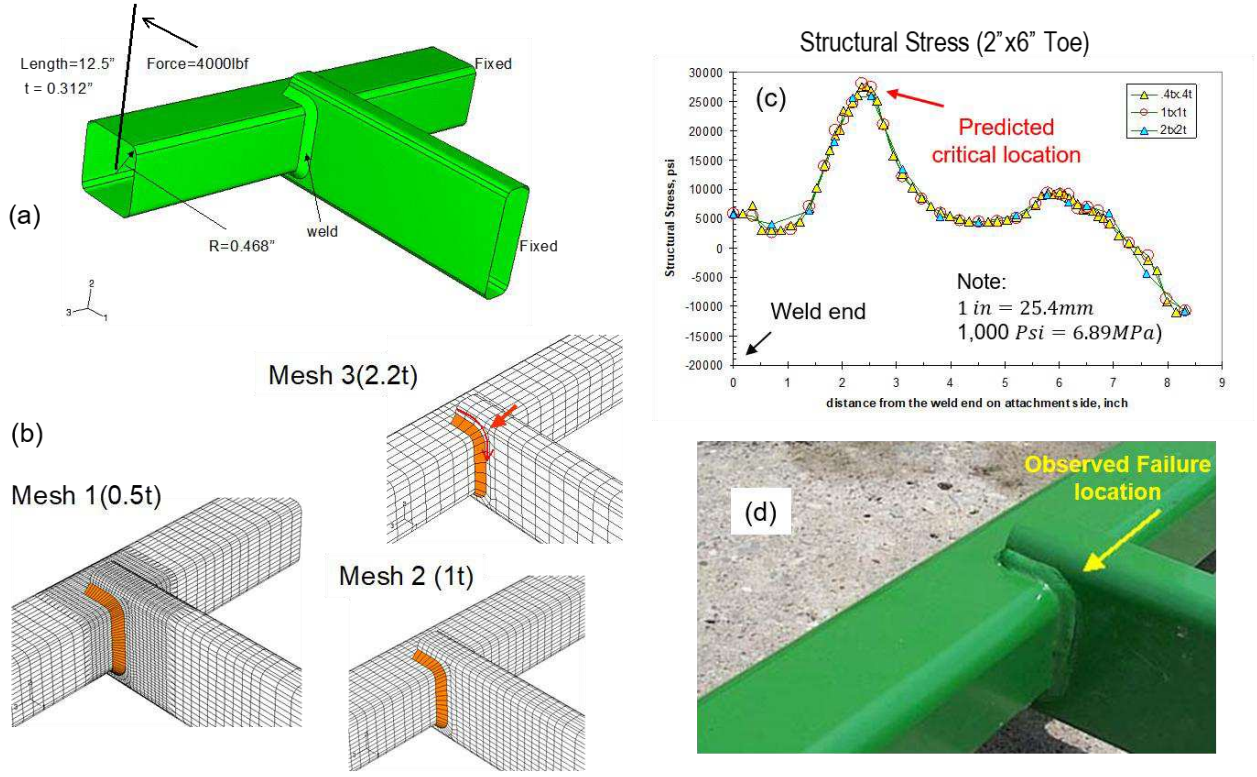


Figure 5: SAE F&DE Committee WELD CHALLENGE problem and mesh-insenstive structural stress results[13]: (a) Test condition; (b) finite element models with different mesh sizes; (c) predicted failure location; (d) actual failure location in tests

In fact, the mesh-insensitivity shown in Figure 5 can be further demonstrated by considering three major commercial FE software packages, e.g., ABAQUS, NASTRAN, and ANSYS, as shown in Figure 6 by using "Mesh 2" in Figure 5. It can be seen that virtually there is no difference in the peak structural value regardless of FE software used. This would not be the case if hot spot stress methods since each FE software outputs local stresses in a different manner, resulting in variability in extrapolated hot spot stress values.

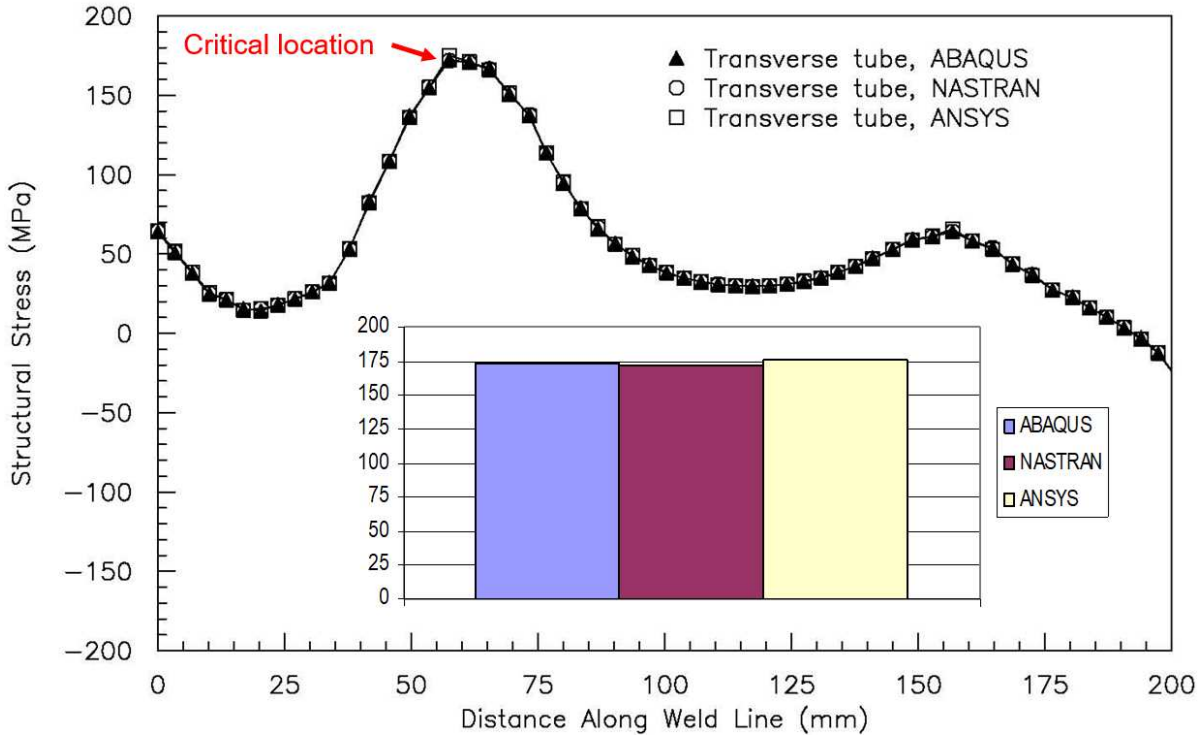


Figure 6: Traction structural stress insensitivity among FE software packages

Another 3D example is an actual ship side shell connection, as shown in Figure 7. IIW 0.4t/1t and 0.5t/1.5t surface stress extrapolation procedures were also used for comparing the mesh-insensitive structural stress method in Figure 7b [14]. Both ABAQUS and NASTRAN with various element types (including Gaussian integration scheme) were evaluated. Element size varies from 1/8t to 2t. The mesh-insensitivity of the structural stress method is evident as shown in Figure 7b[14].

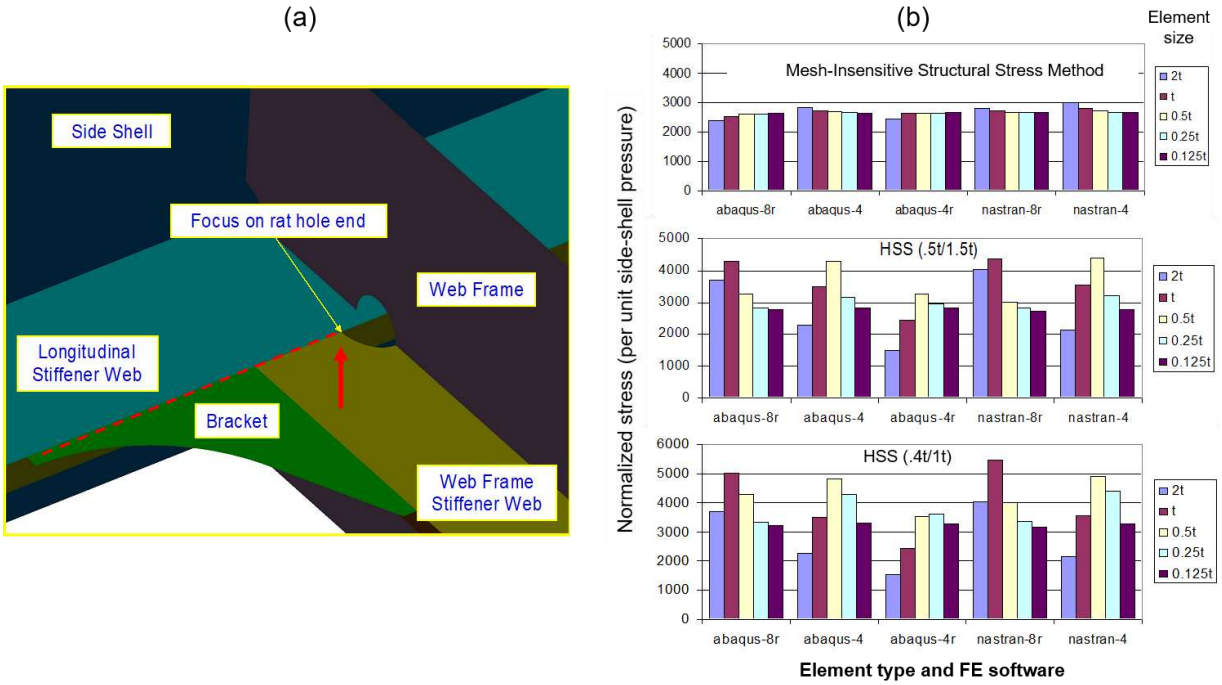


Figure 7: Mesh-insensitive structural stress versus surface extrapolation hot spot stress – a full scale side-shell connnection in a SPSO ship-like structure [14]: (a) side-shell connection geometry and evaluated location indicated by the red arrow line; (b) comparison between the mesh-insenstive structural stress and hot spot stress across different element size and type and ABAQUS versus NASTRAN

3. EQUIVALENT STRUCTURAL STRESS RANGE AND MASTER S-N CURVE

3.1 Equivalent Structural Stress

The structural stress range $\Delta\sigma_s$ is first obtained from the mesh-insensitive structural stress method described in the previous section. It is then converted into an equivalent structural stress range, often expressed in the general form by using fracture mechanics principles [9], [11]:

$$\Delta S_s = \frac{\Delta\sigma_s}{t^{(2-m)/(2m)} I(r)^{1/m}} \tag{6}$$

where:

ΔS_s is the equivalent structural stress range,

$\Delta\sigma_s$ is the structural stress range,

t is plate thickness,

$m = 3.6$ is a fatigue crack growth exponent based on a two-stage crack growth model [11], [15],

$I(r)$ is a dimensionless life integral accounting for loading mode or through-thickness stress gradient,

r is the bending ratio which is expressed as $r = \frac{\Delta\sigma_b}{\Delta\sigma_m + \Delta\sigma_b}$

The dimensionless life integral is represented by a polynomial function after numerical integration using a two-stage crack growth model in [11], as:

$$I(r)^{\frac{1}{m}} = 0.0011 \cdot r^6 + 0.0767 \cdot r^5 - 0.0988 \cdot r^4 + 0.0946 \cdot r^3 + 0.0221 \cdot r^2 + 0.014 \cdot r + 1.2223 \quad (7)$$

The purpose of the equivalent structural stress formulation is to account for the fact that fatigue crack growth is affected by plate thickness and by the through-thickness stress distribution. A membrane-dominated stress field and a bending-dominated stress field with the same surface stress range may not produce the same fatigue crack growth behavior. The function $I(r)$accounts for this difference.

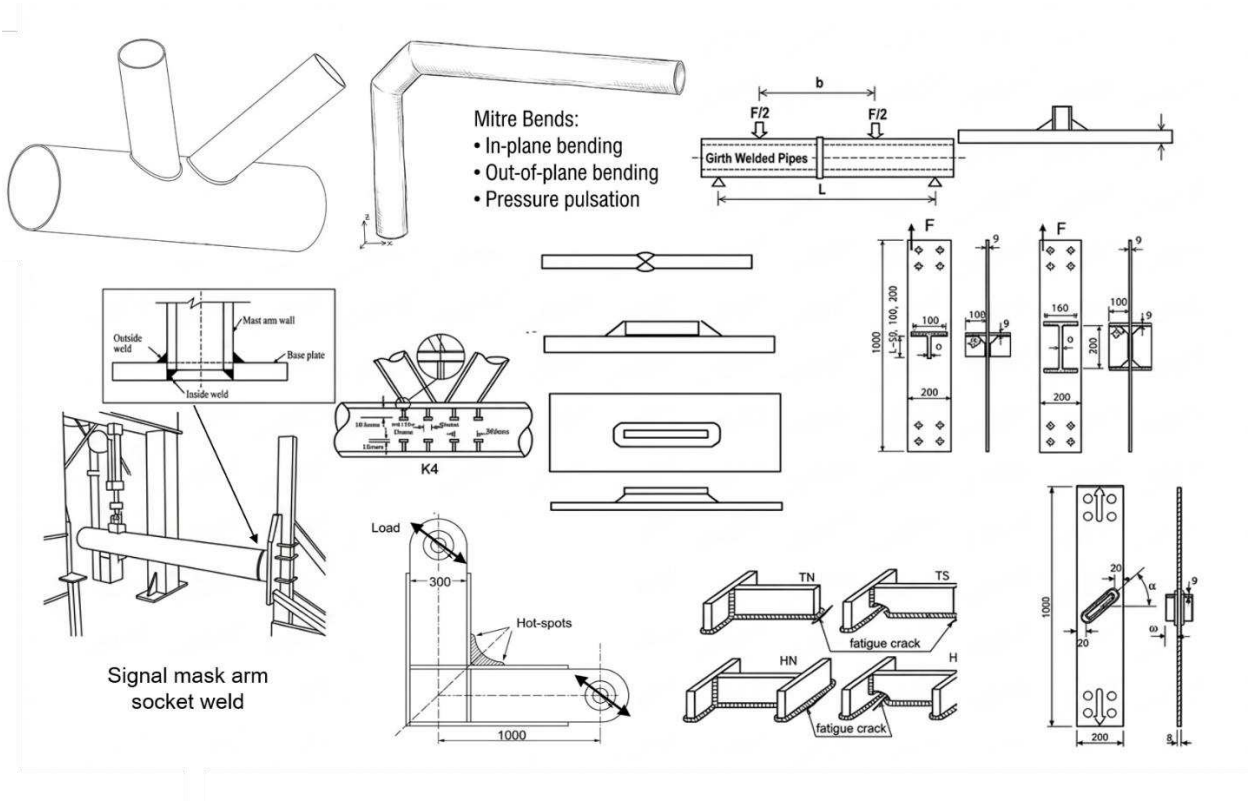


Figure 8: Representatove full-scale and large scale component fatigue tests for validating master S-N curve formulation

3.2 Master S-N Curve Form

The master S–N curve is expressed in ASME BPV Code as [11]:

$$N = C(\Delta S_s)^{-h} \tag{8}$$

or, in logarithmic form:

$$\log N = \log C - h\log \Delta S_s \tag{8a}$$

where:

N is fatigue life in cycles,

ΔS_s is the equivalent structural stress range,

C and h are constants which are determined from welded-joint fatigue data.

By considering a large amount of fatigue test data from full-scale and large-scale components shown in Figure 8, these nominal stress based S-N data (Figure 9a) have been shown to be effectively correlated into a narrow band, as shown in Figure 9b [11] by means of Eqs. (6) and (7). The resulting h in Eq. (8) is given in ASME BPV Code [12] as $h = 0.312$ and $C = 19930$ (mean curve value) and $C = 13876$ (mean minus 2 standard deviations in SI unit for steels, shown by the lines in Figure 10 and Figure 12.

In performing fatigue design evaluation, a design master S–N curve based on either mean minus 2 or 3 standard deviations, depending on Code jurisdiction, can be used to ensure a sufficient conservatism. For instance, ASME BPV Division 2 adopts mean minus 3 standard derivations as its design curve [12].

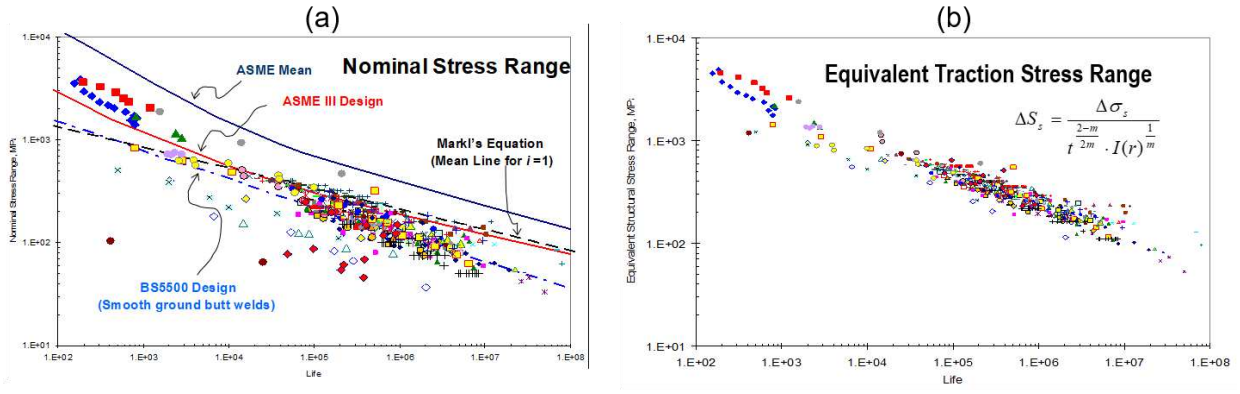


Figure 9: Nominal stress versus mesh-insensitive structural stress range in fatigue test data correlation

3.3 Fatigue Evaluation Procedure

A practical fatigue assessment using the master S–N curve generally follows this sequence:

a. Perform finite element analysis of the welded structure.
b. Identify the weld line and the associated elements on one side of the weld line.

c. Extract nodal forces and moments along the weld line from those elements.
d. Calculate membrane and bending structural stress ranges.
e. Determine the bending ratio r.
f. Calculate the equivalent structural stress range ΔS_s.
g. Use the design master S–N curve (e.g., $mean - 2\sigma$) for calculating design life or $mean \pm 2\sigma$ for test data correlation.
h. For variable-amplitude loading, combine cycle counting with cumulative damage analysis.

For variable-amplitude loading, standard rainflow counting can be directly used to obtain stress range histograms. For multiaxial variable amplitude loading, the path-dependent maximum range (PDMR) cycle counting method [16], [17], [18]. Fatigue damage may then be estimated using Miner's linear damage rule or the newly developed additive damage rule without needing cycle counting [19].

4. REPRESENTATIVE APPLICATIONS

4.1 SAE FD&E Blind Life Prediction

Consider the SAE FD&E Weld Challenge problem described in Figure 5, the structural stress calculated at the peak location in amplitude is at 27Ksi (186MPa) with bending $r = 0.6$. The actual fatigue tests were conducted at remote load ratio of -1. The tube wall thickness at the peak stress location is 8mm. The resulting structural stress range ΔS_s, according to Eq. (6), becomes $\Delta S_s = 502MPa$ [13]. A total of 9 specimens were tested at the same remote load and the results are shown in Figure 10. It can be seen that the mean $\pm 2\sigma$ lines of the master S-N curve provide rather reasonable prediction of these tests.

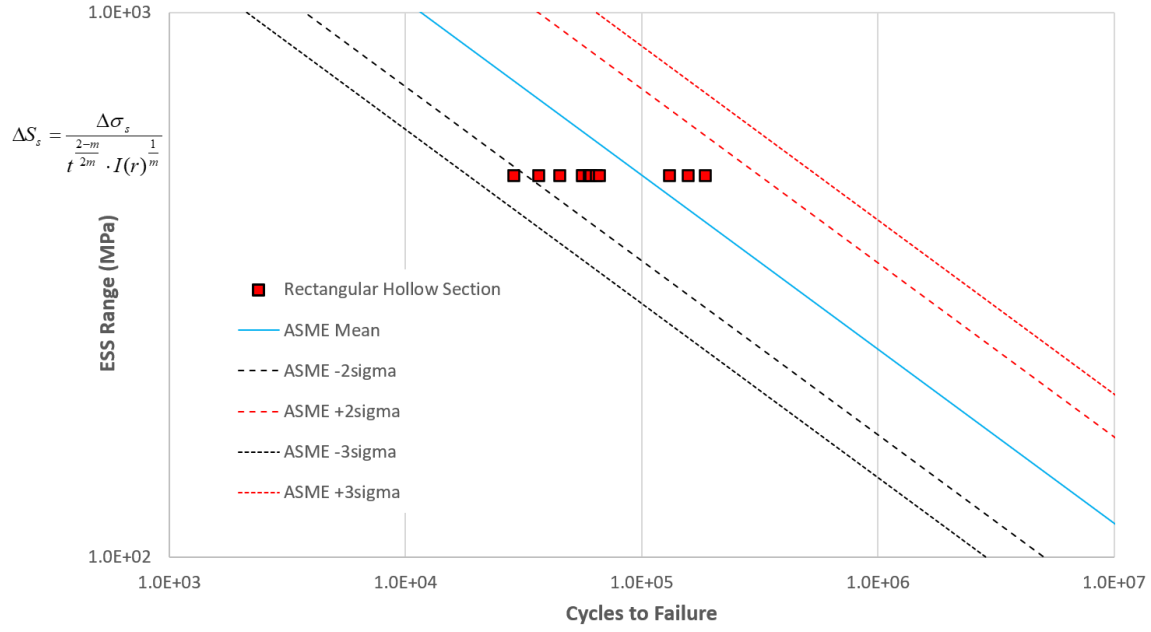


Figure 10: SAE Weld Challenge blind fatigue life prediction using the mesh-insenstive structural stress method and master ASME S-N curve

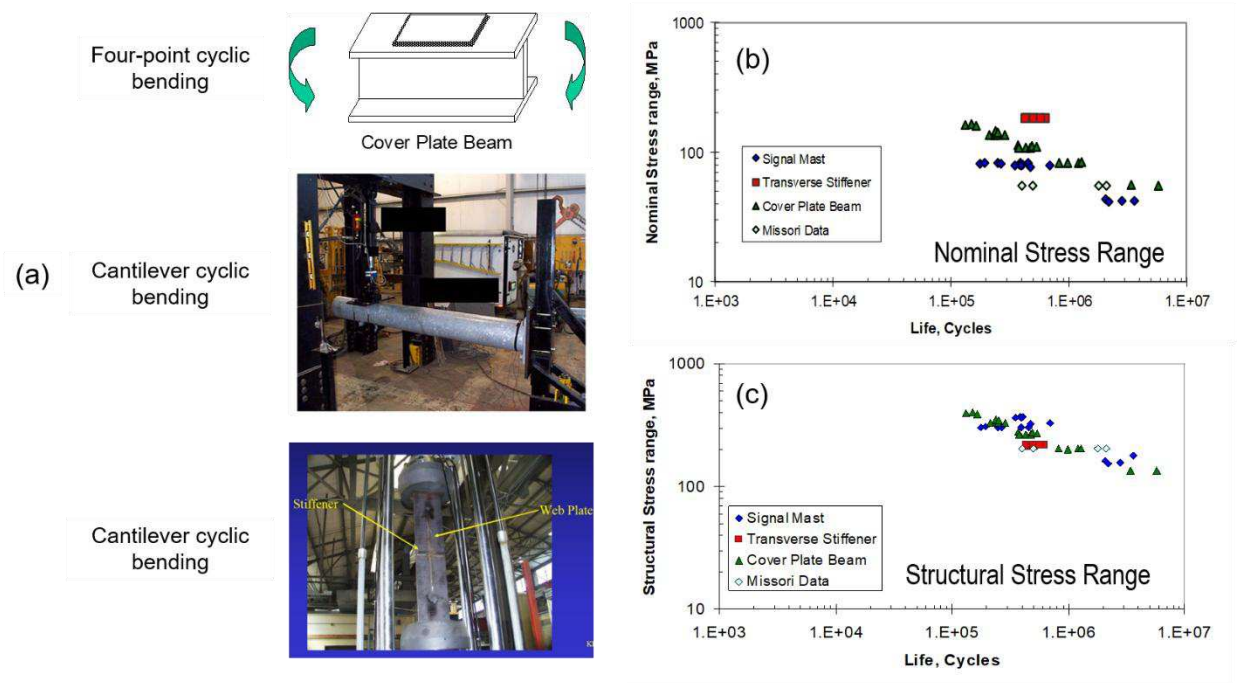


Figure 11: Representative US Department of Transportation (DOT) Full-Scale Fatigue Test Data: (a) Component geometry and test conditions; (b) Test data correlation using nominal stress range; (c) mesh-insensitive structural stress range

4.2 DOT Signal Master Arm Fatigue Tests

US Department of Transportation (DOT) funded a fatigue test initiative to investigate a series of signal mast arm socket weld failures due to the introduction of new design during 2002 through 2005[20] (see Figure 11a). The intention is to identify what Weld Category in AASHTO [21] should be used in fatigue design of these signal mast arm socket welds in comparison with the cover plate fillet weld on I beam flange. The test data analyzed using the classical nominal stress method is shown in Figure 11b. It is worth noting that the test data clearly indicates that there exist three or four data trend lines, as shown in Figure 11b corresponding to different joint configurations shown in Figure 11a. For each test component geometry and loading condition, the mesh-insensitive structural stress is computed. The structural stress range based results in Figure 11c for the same data show that the same data fall into a narrow band without the distinct trend trendlines exhibited in Figure 11b. Once the equivalent structural stress range given in Eq. (6) is used, these data points fall into within master S-N curve mean $\pm 95\%$ scatter band in Figure 12.

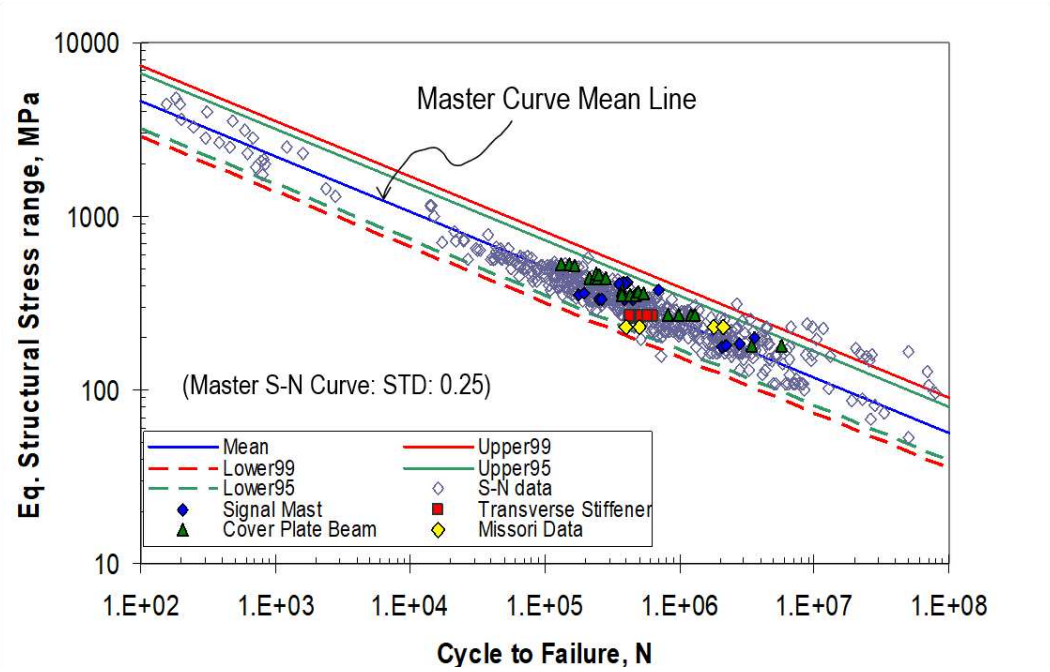
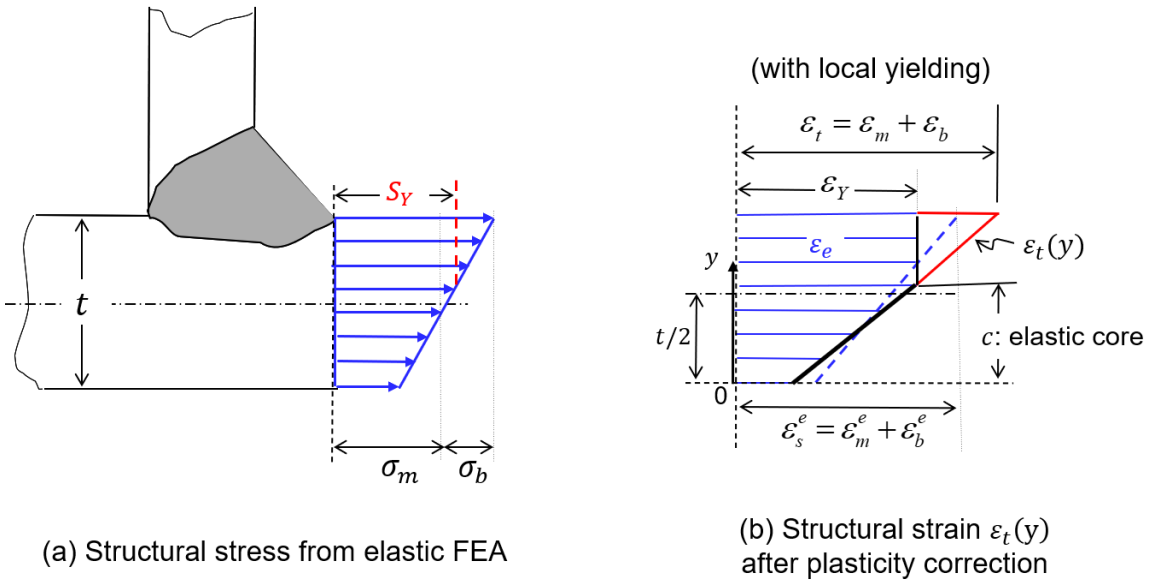


Figure 12: Correlation of DOT full-scale fatigue test data with ASME Master S-N curve scatter band (empty symbols: master S-N curve background data; lines: master S-N curve scatter band measured in standard deviation (STD) of 0.25; color-filled symbols: DOT test data)

5. NATURAL EXTENSION TO STRUCTURAL STRAIN METHOD

5.1. Structural Strain Method

If plastic deformation is no longer negligible , i.e., $\sigma_m + \sigma_b > S_Y$ where S_Y is material yield strength, the mesh-insensitive structural stress discussed so far can be naturally extended to structural strain $\varepsilon_t(y)$, as shown in Figure 13. the structural strain, is simply the linear strain distribution across plate thickness t, consistent with the basic assumption in plate or shell theory, i.e., a cross-thickness plane before deformation remains as a plane after deformation, "plane-remaining-plane" for short. Such an assumption is valid as long as the elastic core c om Figure 13 is larger than zero, i.e., $c > 0$. Then, if plastic deformation is negligible, the structural stress method becomes structural strain method by dividing the structural stresses calculated by Young's modulus E under plane-stress conditions or by $E/(1-v^2)$ under plane-strain conditions with respect to z axis.



(a) Structural stress from elastic FEA

(b) Structural strain $\varepsilon_t(y)$ after plasticity correction

Figure 13: Structural strain as an extension of structural stress definition

By assuming elastic-perfectly-plastic material (i.e., no strain hardening), closed-forms have been developed by considering both loading and unloading (unique to elastic-plastic deformation) [22], [23], [24], [25], [26], [27], [28]. For instance, the structural stress range corresponding stress ratio of 0 can be expressed as [26], [27]:

$$\Delta\varepsilon_t(y) = \frac{[Ky + (S_Y - Kc)]}{E} - (fy + g) \tag{9}$$

where,

$$c = \frac{t}{2}\frac{3(S_Y - \sigma_m) - \sigma_b}{S_Y - \sigma_m}$$

$$f = \frac{K(t-c)^2(t+2c)}{Et^3}$$

$$g = -\frac{K(t-c)^2 c}{Et^2}$$

$$K = \frac{8(S_Y - \sigma_m)^3}{t[3(S_Y - \sigma_m) - \sigma_b]^2}$$

Then, the equivalent structural strain range becomes, according to Eq. (6):

$$\Delta E_s = \frac{\Delta\varepsilon_t(t)}{t^{\frac{2-m}{2m}} \cdot I(r)^{\frac{1}{m}}} \tag{10}$$

Nonlinear strain hardening, e.g., using a modified Ramberg-Osgood stress-strain relationships has also been considered, as discussed in [23], [28].

5.2 Master E-N Curve

With Eq. (10), aluminum alloy, magnesium alloy, and titanium alloy welded connections are also considered, leading to a unified master S-N curve shown in Figure 14 [23].

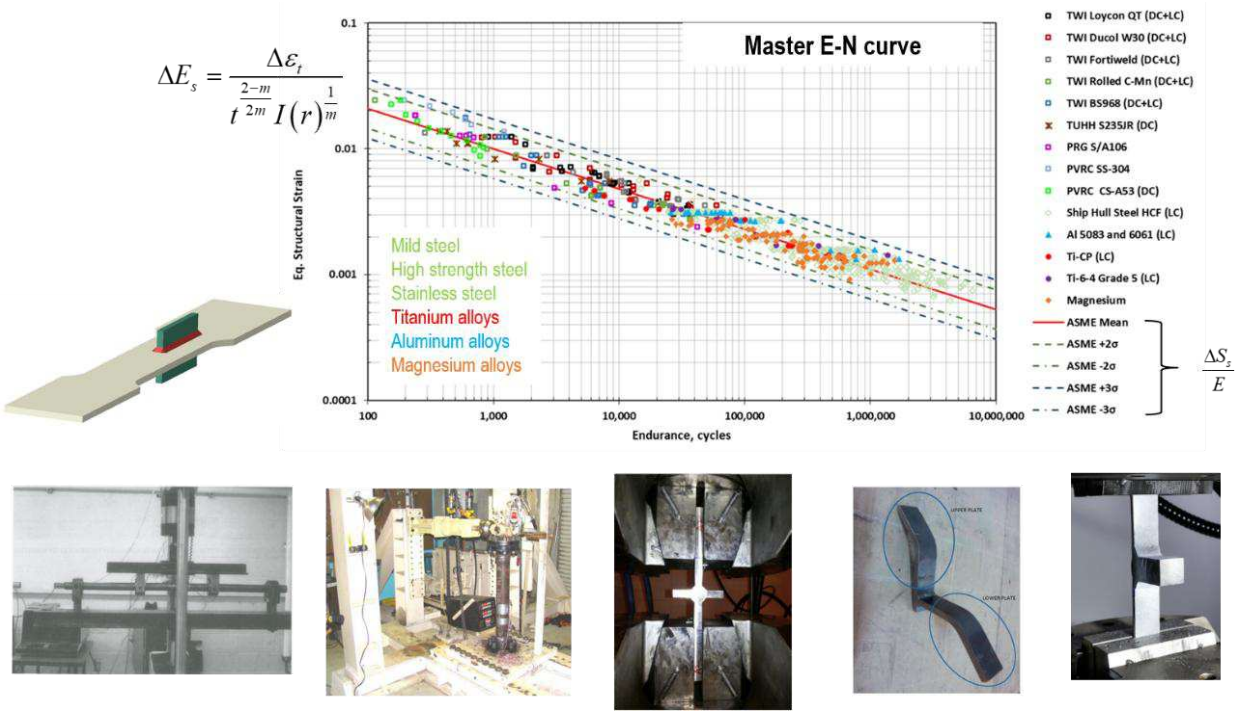


Figure 14: Master E-N curve and its scatter band valdiated by recent fatigue test data of welded components made of different alloys

In the coming API 579-RP/ASME FFS-1 Fitness-for-Service (FFS) code, the structural strain based master E-N curve will replace the master S-N curve for its generality [26], [27], [29].

5.3 Applications for Fatigue Evaluation of Metal AM Components

In fusion-based additive manufacturing for metallic components, due to the presence of solidification-related geometric discontinuities (e.g., see Figure 15a), their fatigue behaviors follow rather similar trends to welded components, based on a series of recent studies [30], [31], [32]. To substantiate such observations, the fatigue test results using notched Inconel 718 AM specimens reported in [33] are summarized in Figure 15. The nominal stress range versus cycles to failure plot of the fatigue test data are shown in Figure 15c. It is interesting to note that the S-N curves are essentially parallel to one another with an inverse slope of about 1/3, sharing a great deal of similarity to the well-recognized S -N curve slope for welded components observed historically [1], [3], [6] and the master S-N curve described in Sec. 3 of this paper.

5.3.1 Mesh-Insensitive Structural Stress Calculation

Since most of the metal AM fatigue testing have been done using small specimens like those shown in Figure 15b. The mesh-insensitive structural stress method described in Sec. 2.2 can be readily adapted for these AM test specimens. Without losing generality, consider typical notched test

specimens shown in Figure 16 [34]. The corresponding traction structural stress definitions are given in Figure 17.

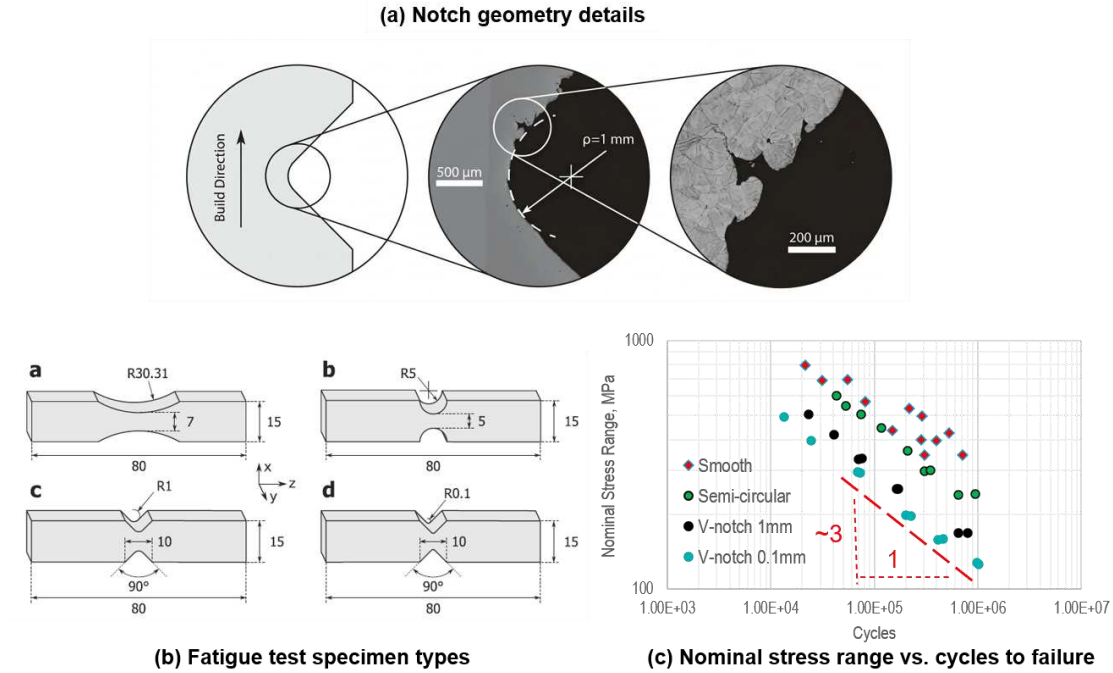


Figure 15: AM fatigue test data from notched specimen by Solbert and Berto (2019) and data correlation using the nominal stress and mesh-insensitive structural stress ranges: (a) Notch tip details; (b) test specimen geometry; (c) fatigue test data - nominal stress range versus cycles to failure.

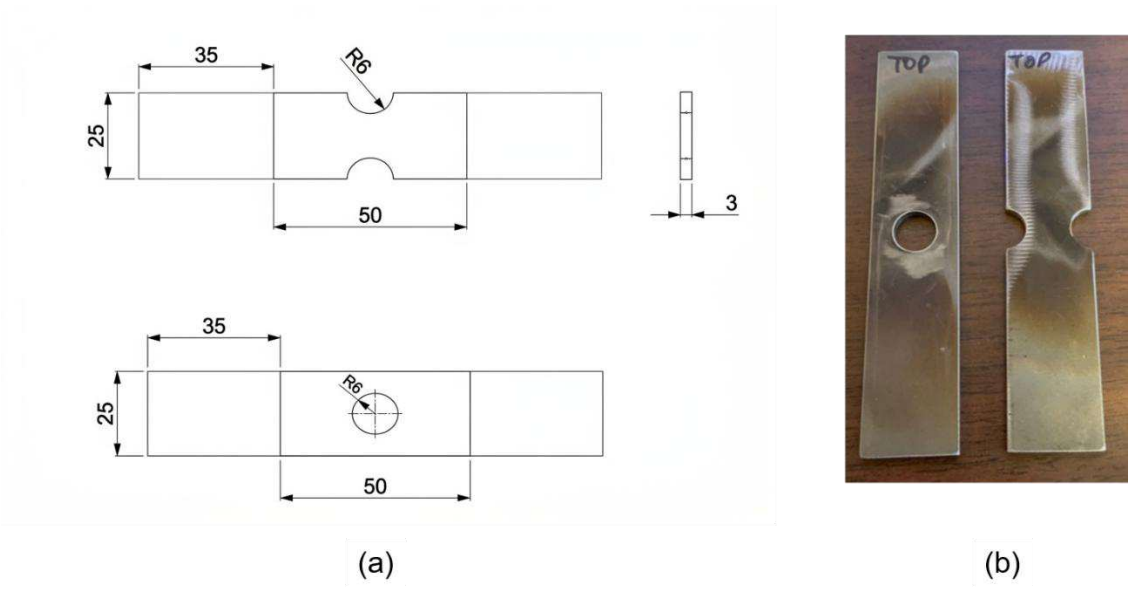


Figure 16: Representee metal AM test specimens with control notch geometry: (a) edge-notched tension (CNT) and center-notched tension (ENT); (b) actual test specimens

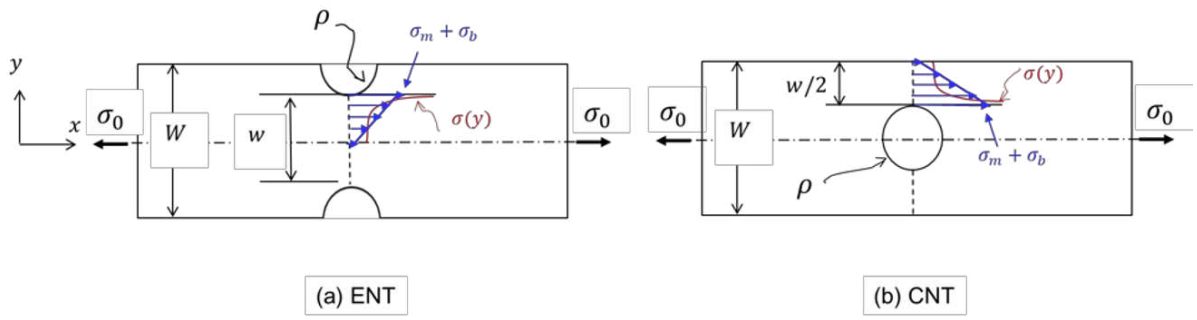


Figure 17: Traction structural stress definitions for edge-notched (ENT) and center-notched (CNT) test specimens

By applying Eq. (2) with respect to the notch tip remaining ligament w and taking advanrage of the symmetry, The membrane and bending parts can then be calculated through:

$$\sigma_m = \frac{1}{w/2}\sum_{i=1}^{n} F_{xi}$$
$$\sigma_b = \frac{6}{(w/2)^2}\sum_{i=1}^{n} F_{xi} \times (y_i - t/2) \qquad (11)$$

where F_{xi} represents the nodal force obtained from the FE results at node i (with $i = 1, n$) in which n is the total number of nodes situated on the line from $y = 0$ to $y = w/2$ at the notch tip, and y_i is nodal position of y at nodal position i. With Eq. (11), the equivalent structural strain range parameter given in Eq. (10) can be determined by dividing $\Delta\sigma_s = \Delta\sigma_m + \Delta\sigma_b$ by Young's modulus for a given AM material. For low-cycle fatigue tests in which displacement-controlled test conditions are used, Eq, (11) gives the pseudo-elastic structural stress for conversion to the structural strain in Eq. (10).

When analyzing specimens with axisymmetry (i.e., round bar specimens under cyclic tension or compression), F_{xi} is simply replaced by $F_{xi}/2\pi y_i$ in Eq. (11) since in FE computation for axisymmetric models the nodal forces represent the total ring forces at a given radial distance y_i.

5.3.2 AM Test Data Correlation

In supporting ASME BPV Code Case (Case Record No. 22-1598), an extensive literature collection of metal AM fatigue has been analyzed [30], [31], [34] using the structural stress method embodied by Eq. (11) and the master E-N curve approach described in Sec. 5.2. A representative collection of fatigue specimen geometries (most tested under cyclic tension and some tested under cyclic bending) are shown in Figure 18. The fatigue test data are plotted in Figure 19a in terms of nominal strain range. It can be seen than the data scatter is significant with a standard deviation of $\sigma = 0.53$. Once the equivalent structural strain range given in Eq. (10) is used, not only are the data from different materials and test specimen geometries are consolidated into a narrow band, but also are

largely situated within the master E-N curve scatter band (lines in Figure 19b). Note that a few data points out of the data set labeled as "SS316L (UST)" were tested under ultrasonic frequency which may introduce some uncertainty. Some further investigation on this set of the data is currently on-going.

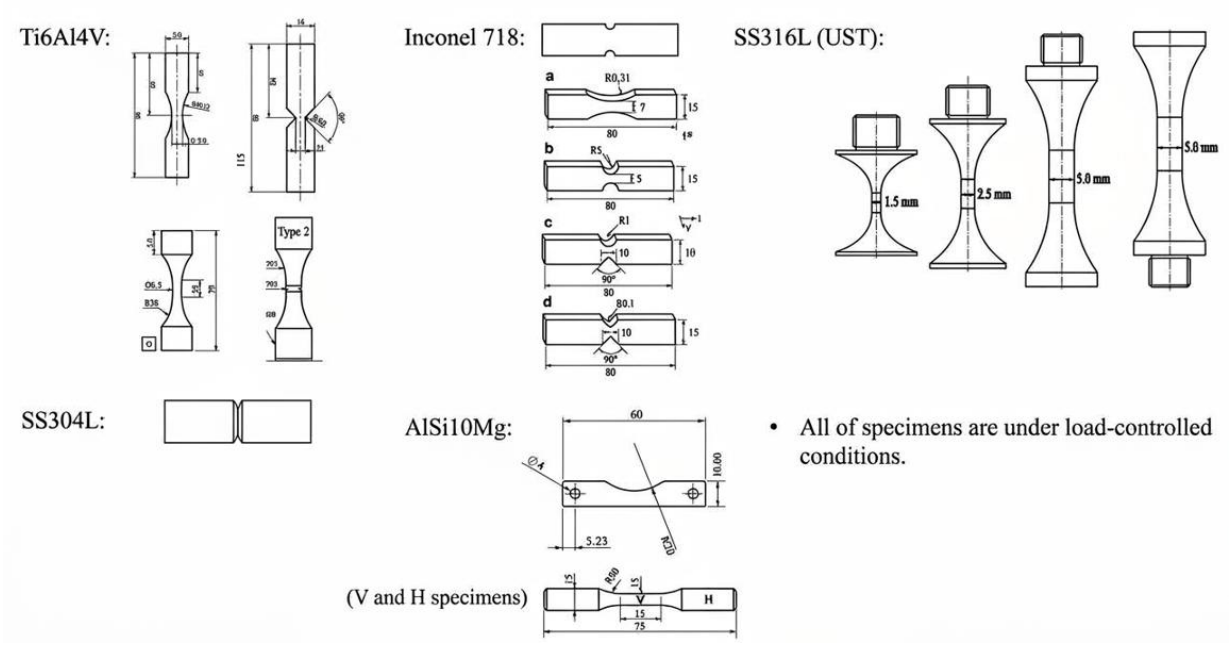


Figure 18: Representative AM fatigue specimens and materials analyzed by the structural strain method for supporting ASME BPV Code Case (Case Record No. 22-1598)

5.4 Other Related Developments

There are other related developments for extending the mesh-insensitive method's applications. These include:

- Multiaxial cycle fatigue evaluation method: fatigue damage parameter formulation and cycle counting method, including further extension of the path-depending maximum range (PDMR) cycle techniques and frequency domain implementation of PDMR method [16], [17], [18]
- Additive fatigue damage accumulation model without needing cycle counting [32]
- Treatment dissimilar material joints: incompatible metal to metal joints (e.g., aluminum to steel, aluminum to copper, and polymer to metal joints) [35], [36]
- User-element (UEL) method for eliminating the needs for representing welds/joints when evaluating complex structures[32], [33], [34], which has been considered as a limitation of

the method since it is typically required to represent overall weld geometry (e.g., fillet weld in Figure 5.

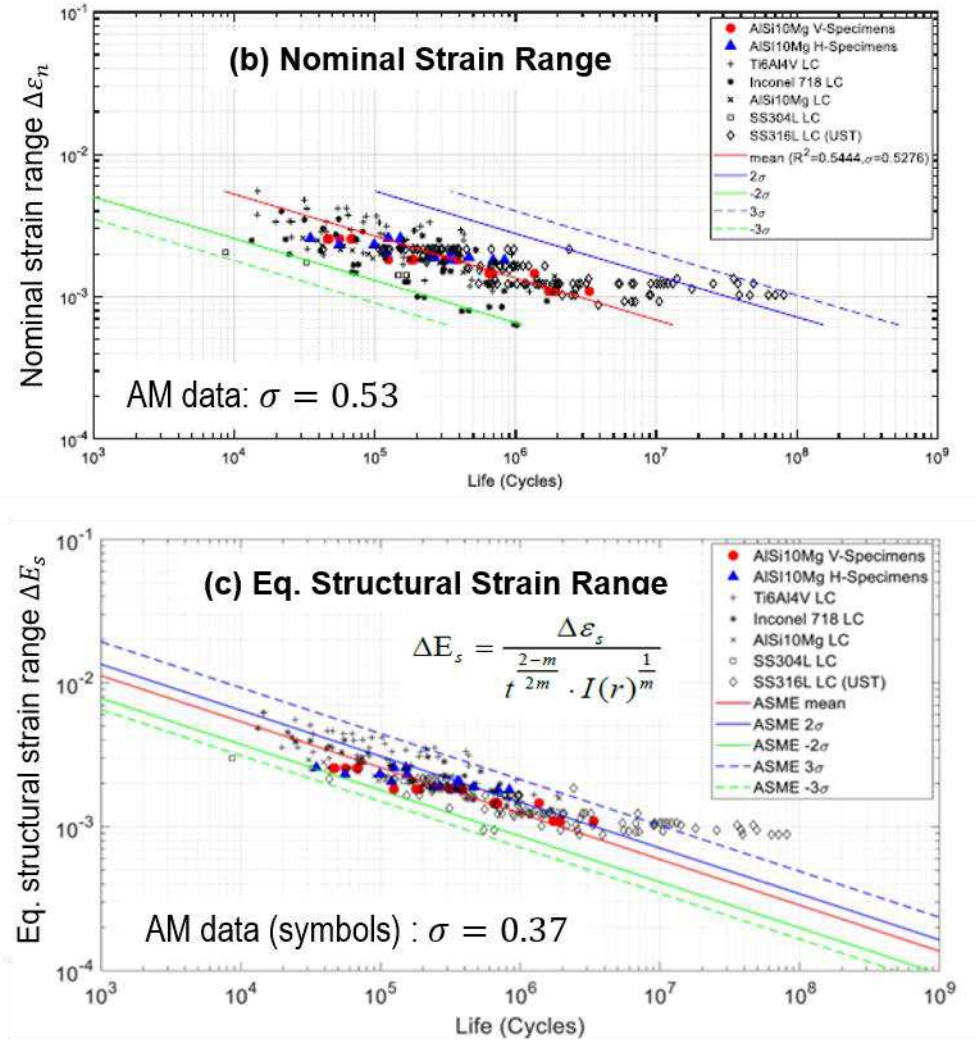


Figure 19: Structural strain based AM fatigue test correlation with the master E-N curve and its scatter band: (a) nominal strain range; (b) equivalent structural strain range

5 CONCLUSIONS

This paper is only intended to provide a broad stroke overview of the mesh-intensive structural stress method and its most recent applications and original contributions, but also its mechanics under pinning, i.e., far-field traction stress at a hypothetical crack location, e.g., at weld location. Such traction-based structural stresses can be more consistently computed by using nodal forces and nodal moments from FEA outputs, rather than using local stresses. Therefore, the difference

in calculation procedure can be viewed as somewhat complicated than legacy surface extrapolation based hot spot stress methods. This can be viewed as a limitation of this method. Another one is the lack of general measurement method since the traction structural stress parameter requires the access to both plate surfaces [37]. The recent developments highlighted in Sec. 5.4 are intended to address some of concerns. Recognizing some of the further development needs, the following key features of the mesh-insensitive method demonstrated so far are worth noting:

a) The mesh-insensitive structural stress method addresses the singularity issues in fatigue evaluation of welded components by calculating fatigue-relevant stress from nodal forces and moments that satisfy equilibrium through a novel matrix equation relating nodal forces and nodal moments to line forces and line moments
b) The resulting master S–N curve approach uses equivalent structural stress to correlate fatigue data from a wide range of welded joint types, leading to a consolidated fatigue S-N curve and its scatter band.
c) Since its adoption by the ASME Boiler and Pressure Vessel Code in 2007, the method has become an important tool for engineering fatigue assessment of pressure equipment and welded components.
d) The structural strain based Master E-N Curve method as a natural extension of the structural stress method offers a unified treatment not only from low cycle to high cycle fatigue regime, but also among welded connections made of different base materials varying from steel to aluminum to titanium alloys.
e) Recent developments proved that the master E-N curve method is effective for correlating metal AM component fatigue test data and offers a quantitative means for extracting fatigue design allowables for avoiding exhaustive fatigue testing.

DECLARATIONS

Competing Interests: The author declares no competing interests.

Funding: This work was supported by the Office of Naval Research under Grant No. N000-14-26-1-2306.

REFERENCES

[1] T. R. Gurney, *Fatigue of welded structures*. CUP Archive, 1979.

[2] S. J. Maddox, *Fatigue strength of welded structures*. Woodhead publishing, 1991.

[3] S. Maddox, “Fatigue design rules for welded structures,” in *Fracture and fatigue of welded joints and structures*, Elsevier, 2011, pp. 168–207.

[4] W. Fricke, “Recommended hot-spot analysis procedure for structural details of ships and FPSOs based on round-robin FE analyses,” *International Journal of Offshore and Polar Engineering*, vol. 12, no. 01, 2002.

[5] W. Fricke, “Fatigue analysis of welded joints: state of development,” *Marine structures*, vol. 16, no. 3, pp. 185–200, 2003.

[6] A. Hobbacher, *Recommendations for fatigue design of welded joints and components*, vol. 47. Springer, 2016.

[7] J. Baumgartner, A. F. Hobbacher, and R. Rennert, “Fatigue assessment of welded thin sheets with the notch stress approach – Proposal for recommendations,” *International Journal of Fatigue*, vol. 140, p. 105844, Nov. 2020, doi: 10.1016/j.ijfatigue.2020.105844.

[8] P. Dong, “A Structural Stress Definition and Numerical Implementation for Fatigue Evaluation of Welded Joints,” *International Journal of Fatigue*, vol. 23, no. 10, pp. 865–876, 2001.

[9] P. Dong, “A robust structural stress method for fatigue analysis of offshore/marine structures,” *J. Offshore Mech. Arct. Eng.*, vol. 127, no. 1, pp. 68–74, 2005.

[10] P. Dong and J. K. Hong, “The Master S-N Curve Approach to Fatigue of Piping and Vessel Welds,” *Weld World*, vol. 48, no. 1, pp. 28–36, Jan. 2004, doi: 10.1007/BF03266411.

[11] P. Dong, J. Hong, D. Osage, D. Dewees, and M. Prager, “The master SN curve method: an implementation for fatigue evaluation of welded components in the ASME B&PV Code, Section VIII, Division 2 and API 579-1/ASME FFS-1,” *Welding Research Council Bulletin*, no. 523, 2010.

[12] ASME B&PV Code Committee, *The 2007 ASME Boiler and Pressure Vessel (B&PV) Code, Section VIII, Division 2*, 2007.

[13] H. Kyuba and P. Dong, “Equilibrium-equivalent structural stress approach to fatigue analysis of a rectangular hollow section joint,” *International Journal of Fatigue*, vol. 27, no. 1, pp. 85–94, 2005.

[14] B. E. Healy, “A case study comparison of surface extrapolation and Battelle structural stress methodologies,” presented at the International Conference on Offshore Mechanics and Arctic Engineering, 2004, pp. 447–464.

[15] P. Dong, J. Hong, and Z. Cao, “Stresses and stress intensities at notches:‘anomalous crack growth’revisited,” *International journal of fatigue*, vol. 25, no. 9–11, pp. 811–825, 2003.

[16] P. Dong, Z. Wei, and J. K. Hong, “A path-dependent cycle counting method for variable-amplitude multi-axial loading,” *International Journal of Fatigue*, vol. 32, no. 4, pp. 720–734, 2010.

[17] J. Mei and P. Dong, “A new path-dependent fatigue damage model for non-proportional multi-axial loading,” *International Journal of Fatigue*, vol. 90, pp. 210–221, 2016.

[18] Z. Wei, P. Dong, J. Mei, X. Pei, and S. K. Ravi, “A moment of load path-based parameter for modeling multiaxial fatigue damage of welded structures,” *International Journal of Fatigue*, vol. 171, p. 107575, 2023.

[19] Z. Wei and P. Dong, “An additive fatigue damage accumulation modeling procedure without Needing cycle counting,” *International Journal of Fatigue*, p. 109716, 2026.

[20] M. T. Koenigs, T. A. Botros, D. Freytag, and K. H. Frank, “Fatigue strength of signal mast arm connections,” U.S. Department of Transportation Federal Highway Administration, FHWA/TX-04/4178-2, 2003.

[21] AASHTO, “AASHTO LRFD Bridge Construction Specification,” 2017.

[22] P. Dong, X. Pei, S. Xing, and M. Kim, “A structural strain method for low-cycle fatigue evaluation of welded components,” *International Journal of Pressure Vessels and Piping*, vol. 119, pp. 39–51, 2014.

[23] X. Pei and P. Dong, “An analytically formulated structural strain method for fatigue evaluation of welded components incorporating nonlinear hardening effects,” *Fatigue & Fracture of Engineering Materials & Structures*, vol. 42, no. 1, pp. 239–255, 2019.

[24] X. Pei, P. Dong, and S. Xing, “A structural strain parameter for a unified treatment of fatigue behaviors of welded components,” *International Journal of Fatigue*, vol. 124, pp. 444–460, 2019.

[25] X. Pei, P. Dong, and M. H. Kim, “A simplified structural strain method for low-cycle fatigue evaluation of girth-welded pipe components,” *International Journal of fatigue*, vol. 139, p. 105732, 2020.

[26] Z. Wei, P. Dong, and X. Pei, “The Structural Strain Method for Fatigue Evaluation of Welded Components: Closed-Form Solutions,” *International Journal of Fatigue*, p. 108119, 2023.

[27] Z. Wei, L. Lei, X. Pei, and P. Dong, “The structural strain method for fatigue evaluation of welded components: Analytical treatment of reversed plasticity,” *International Journal of Pressure Vessels and Piping*, vol. 210, p. 105249, 2024.

[28] X. Pei, X. Li, S. Zhao, P. Dong, X. Liu, and M. Xie, “Low cycle fatigue evaluation of welded structures with arbitrary stress-strain curve considering stress triaxiality effect,” *International Journal of Fatigue*, vol. 162, p. 106969, 2022.

[29] P. Dong, Z. Wei, X. Pei, and D. Osage, *Structural Strain Method: A Unified Structural Fatigue Evaluation Procedure from the Low-Cycle to High-Cycle Fatigue Regime*, The 1st Edition. in WRC Bulletin, no. 610. Welding Research Council (WRC), 2026. [Online]. Available: https://store.accuristech.com/wrc/searches/67922548

[30] S. Wu and P. Dong, “Modeling of distributed defects and a proposed fatigue interaction criterion for additively manufactured metal parts,” *International Journal of Pressure Vessels and Piping*, p. 105048, 2023.

[31] P. Dong, G. Rawls, and T. Krentz, “Fatigue property evaluation of metallic AM parts and determination of design stress allowables,” presented at the Pressure Vessels and Piping Conference, American Society of Mechanical Engineers, 2023, p. V001T01A074.

[32] Z. Jin and P. Dong, “A reduced-order modelling procedure for estimating residual stress and distortion in fusion-based metal AM parts,” *Additive Manufacturing*, vol. 109, p. 104856, Jul. 2025, doi: 10.1016/j.addma.2025.104856.

[33] K. Solberg and F. Berto, “Notch-defect interaction in additively manufactured Inconel 718,” *International Journal of Fatigue*, vol. 122, pp. 35–45, 2019.

[34] T. Krentz, P. Dong, and G. Rawls, “Characterization of Fatigue Behaviors of Notched 316L DED AM Specimens,” presented at the ASME 2024 Pressure Vessels & Piping Conference, American Society of Mechanical Engineers Digital Collection, Nov. 2024. doi: 10.1115/PVP2024-123384.

[35] Y. Zhang and P. Dong, “An elastic foundation modeling approach to bi-material interface crack problems of finite bond length,” *Theoretical and Applied Fracture Mechanics*, vol. 138, p. 104933, Aug. 2025, doi: 10.1016/j.tafmec.2025.104933.

[36] Y. Zhang, P. Dong, and X. Pei, “Fracture mechanics modeling of fatigue behaviors of adhesive-bonded aluminum alloy components,” *Metals*, vol. 12, no. 8, p. 1298, 2022.

[37] M. Kim and S. Kang, “Testing and analysis of fatigue behaviour in edge details: a comparative study using hot spot and structural stresses,” *Proceedings of the Institution of Mechanical Engineers, Part C: Journal of Mechanical Engineering Science*, vol. 222, no. 12, pp. 2351–2363, 2008.